


## Debye-screening effect on electron-impact excitation of helium-like $Al^{11+}$ and $Fe^{24+}$ ions

Yu-Long Ma(马玉龙), Ling Liu(刘玲), Lu-You Xie(颉录有), Yong Wu(吴勇), Deng-Hong Zhang(张登红), Chen-Zhong Dong(董晨钟), Yi-Zhi Qu(屈一至), and Jian-Guo Wang(王建国)

**Citation:**Chin. Phys. B, 2022, 31 (**4**): 043401. DOI: 10.1088/1674-1056/ac2e65
Journal homepage: http://cpb.iphy.ac.cn; http://iopscience.iop.org/cpb

**What follows is a list of articles you may be interested in**

---

## Electron-impact ionization cross section calculations for lithium-like ions

Guo-Jie Bian(卞国杰), Jyh-Ching Chang(张稚卿), Ke-Ning Huang(黄克宁), Chen-Sheng Wu(武晨晟), Yong-Jun Cheng(程勇军), Kai Wang(王凯), and Yong Wu(吴勇)

Chin. Phys. B, 2022, 31 (**1**): 013401. DOI: 10.1088/1674-1056/ac229e

## Electron-impact single ionizaiton for $W^{4+}$ and $W^{5+}$

Denghong Zhang(张登红), Luyou Xie(颉录有), Jun Jiang(蒋军), Zhongwen Wu(武中文), Chenzhong Dong(董晨钟), Yinglong Shi(师应龙), Yizhi Qu(屈一至)

Chin. Phys. B, 2018, 27 (**5**): 053402. DOI: 10.1088/1674-1056/27/5/053402

## Analysis of the fractal intrinsic quality in the ionization of Rydberg helium and lithium atoms

Yanhui Zhang(张延惠), Xiulan Xu(徐秀兰), Lisha Kang(康丽莎), Xiangji Cai(蔡祥吉), Xu Tang(唐旭)

Chin. Phys. B, 2018, 27 (**5**): 053401. DOI: 10.1088/1674-1056/27/5/053401

## Production of projectile and target *K*-vacancy in near-symmetric collisions of 60-100 MeV $Cu^{9+}$ ions with thin Zn target

Yipan Guo(郭义盼), Zhihu Yang(杨治虎), Shubin Du(杜树斌), Hongwei Chang(常宏伟), Qingliang Xia(夏清良), Qiumei Xu(徐秋梅)

Chin. Phys. B, 2016, 25 (**3**): 033401. DOI: 10.1088/1674-1056/25/3/033401

## Fast-electron-impact ionization process by 3p of hydrogen-like ions in Debye plasmas

Qi Yue-Ying, Ye Dan-Dan, Wang Jian-Guo, Qu Yi-Zhi

Chin. Phys. B, 2015, 24 (**3**): 033403. DOI: 10.1088/1674-1056/24/3/033403

---

# Debye-screening effect on electron-impact excitation of helium-like $Al^{11+}$ and $Fe^{24+}$ ions

Yu-Long Ma(马玉龙)[1,2], Ling Liu(刘玲)[2,†], Lu-You Xie(颉录有)[1], Yong Wu(吴勇)[2,3,‡], Deng-Hong Zhang(张登红)[1], Chen-Zhong Dong(董晨钟)[1], Yi-Zhi Qu(屈一至)[4], and Jian-Guo Wang(王建国)[2]

[1] *College of Physics and Electronic Engineering, Northwest Normal University, Lanzhou* 730070, *China*
[2] *Key Laboratory of Computational Physics, Institute of Applied Physics and Computational Mathematics, Beijing* 100088, *China*
[3] *Center for Applied Physics and Technology, Peking University, Beijing* 100084, *China*
[4] *School of Optoelectronics, University of Chinese Academy of Sciences, Beijing* 100049, *China*

(Received 26 July 2021; revised manuscript received 23 September 2021; accepted manuscript online 11 October 2021)

Debye-screening effects on the electron-impact excitation (EIE) processes for the dipole-allowed transition $1s^2\ {}^1S \rightarrow 1s2p\ {}^1P$ in He-like $Al^{11+}$ and $Fe^{24+}$ ions are investigated using the fully relativistic distorted-wave methods with the Debye–Hückel (DH) model potential. Debye-screening effects on the continuum-bound (CB) interaction and target ion are discussed, both of which result in reduction of EIE cross sections. This reduction due to screening on the CB interaction is dominant. The non-spherical and spherical DH potentials are adopted for considering the screening effect on the CB interaction. It is found that the spherical DH potential could significantly overestimate the influence of plasma screening on EIE cross sections for multielectron He-like ions.

**Keywords:** Debye plasmas, electron-impact excitation, Debye–Hückel model potential, He-like $Al^{11+}$ and $Fe^{24+}$ ions

**PACS:** 34.50.Fa, 52.20.–j, 52.20.Fs **DOI:** 10.1088/1674-1056/ac2e65

## 1. Introduction

Electron-impact excitation (EIE) processes in various plasmas have been subject to continued interest due to their potential application. For example, EIE cross sections are required for calculating the spectral line intensities and especially level populations of nonlocal-thermodynamic-equilibrium (NLTE) plasmas.[1,2] Line emissions from the excited states produced by the EIE process provide valuable information on plasma parameters such as temperature and density.[3,4] Theoretical studies on electron–ion collision processes are needed to consider screening effects due to plasma environments, covering both weakly and strongly coupled plasmas. The electron–ion interaction in the strongly coupled plasmas is often described by the ion-sphere model potential.[5–8] For weakly coupled (or Debye) plasmas, the Debye–Hückel (DH) potential[9–12] of an ion of positive charge $Z$ which interacts with an electron is given by

$$V(r) = -\frac{Ze^2}{r}\exp\left(-\frac{r}{D}\right), \tag{1}$$

where $D = (k_B T_e/4\pi e^2 n_e)^{1/2}$ is the Debye screening length, $T_e$ and $n_e$ are the electron temperature and density, respectively, and $k_B$ is the Boltzmann constant. It is noted that when the Coulomb coupling parameter $\Gamma = e^2/\bar{a}k_B T_e \ll 1$ the Debye-screening potential (1) is valid, where $\bar{a} = (3/4\pi n_e)^{1/3}$ is the average distance between particles.

When a continuum electron interacts with ions that are immersed in Debye plasmas, two types of DH potentials[12,13] are employed to describe the interaction between the continuum electron and bound electron of the target ion, referred to as the continuum-bound (CB) interaction for simplicity, in an electron–ion collision. The first one is a non-spherical DH (NSDH) potential[12]

$$V(\boldsymbol{r}_1, \boldsymbol{r}_2) = \frac{1}{|\boldsymbol{r}_1 - \boldsymbol{r}_2|}\exp\left(-\frac{|\boldsymbol{r}_1 - \boldsymbol{r}_2|}{D}\right), \tag{2}$$

which includes the screening on both the continuum electron and bound electron of the target ion. In Eq. (2), $\boldsymbol{r}_1$ and $\boldsymbol{r}_2$ are the coordinates of the bound electron and continuum electron, respectively. It is noted that this NSDH potential has also been adopted for positron–ion collision in Debye plasmas.[14,15]

In contrast to the NSDH potential of Eq. (2), the screened CB interaction is expressed by the spherical DH (SDH) potential[12]

$$V(\boldsymbol{r}_1, \boldsymbol{r}_2) = \frac{1}{|\boldsymbol{r}_1 - \boldsymbol{r}_2|}\exp\left(-\frac{|\boldsymbol{r}_2|}{D}\right). \tag{3}$$

Due to its spherical symmetry, the SDH potential is well suited to atomic calculations. Therefore, a significant number of theoretical studies have also been devoted to electron- and proton-impact excitation processes based on the SDH potential. The first attempt at using the SDH model was made by Hatton *et al.*[16] for the study of inelastic scattering of

†Corresponding author. E-mail: liu_ling@iapcm.ac.cn
‡Corresponding author. E-mail: wu_yong@iapcm.ac.cn

© 2022 Chinese Physical Society and IOP Publishing Ltd 

H-like ions in a dense plasma. Later, the Debye-screened impact cross sections were calculated for H-like ions by using the Born approximation and close-coupling methods,[7] semiclassical impact-parameter formalism[17] and relativistic distorted-wave (RDW) method,[18] as well as for He-like ions by using the RDW method.[19–21] Moreover, the Debye-screening effect on the electron-impact ionization of H-like ions[22] and multielectron $Ne^{4+}$ and $Au^{47+}$ ions has been studied with the SDH potential.[23]

Yoon and Jung[13] have performed a comparison of the Debye-screened behavior between the SDH and NSDH potentials for the EIE process of H-like ions. They suggested that the NSDH model is physically more reliable, but only calculated the transition probabilities. To the best of our knowledge, such comparisons have not yet been performed for the EIE cross sections of multielectron ions. Therefore, the motivation of the present study is to present a detailed analysis and comparison of cross sections between NSDH and SDH model potentials that are used to describe the Debye-screened CB interaction for the EIE of multielectron ions.

Apart from the plasma screening on the CB interaction, plasma screening imposed on the target ion will also affect the EIE cross sections. Zhang *et al.*[24–26] studied the Debye-screening effect on low-energy electron–H scattering using the R-matrix method with pseudostates. Zammit *et al.*[27–29] also calculated the excitation and ionization cross sections of electron–H/He-atom collisions in Debye plasmas by the convergent close-coupling (CCC) method. They have naturally included the Debye screening on the target ion when the DH potentials for the electron–electron and electron–nucleus interactions are adopted in the $(N+1)$-electron Hamiltonian, but the influence of the Debye screening imposed on the target ion on the cross sections has not been discussed. Therefore, the influence of the Debye screening imposed on the target ion on the EIE cross section are investigated in the present work.

We shall restrict our discussions to the simplest multielectron system of He-like ions such as $Al^{11+}$ and $Fe^{24+}$, but it can be extended to other complex ions straightforwardly. Specifically, the dipole-allowed transition $1s^2\ {}^1S \rightarrow 1s2p\ {}^1P$ is discussed, as this line of atomic systems embedded in plasmas is often investigated to test various models that have been developed to describe the plasma screening effects.[30,31] To obtain the EIE cross sections, we performed fully relativistic multiconfiguration Dirac–Fock (MCDF) and RDW calculations.

## 2. Theoretical methods

We briefly present the RDW method for calculating the EIE cross sections (please refer to Refs. [32–34] for more details). The EIE cross section $\sigma_{\rm if}$ from initial state 'i' to final state 'f' is expressed in terms of the collision strength $\Omega_{\rm if}$ as[33]

$$\sigma_{\rm if} = \frac{\pi}{k_{\rm i}^2 g_{\rm i}} \Omega_{\rm if}, \tag{4}$$

where $g_{\rm i}$ is the statistical weight of the initial state, and $k_{\rm i}$ is the kinetic momentum of the incident continuum electron. The collision strength is given by[33]

$$\Omega_{ij} = 2\sum_{J_{\rm T}} (2J_{\rm T}+1) \sum_{\kappa_{\rm i},\kappa_{\rm f}} \left| \langle \Psi_{\rm i} | \sum_{p<q}^{N+1} \frac{1}{r_{pq}} | \Psi_{\rm f} \rangle \right|^2, \tag{5}$$

where $\kappa_{\rm i}$ and $\kappa_{\rm f}$ are the initial and final relativistic quantum numbers for the continuum electron, respectively. $\Psi$ represents the antisymmetric wavefunctions for the total $(N+1)$-electron system with total angular momentum $J_{\rm T}$, which consists of the incident (or scattered) continuum electron and the bound target wavefunction.

In the practical RDW calculations, the Coulomb potential between electrons is expanded in the partial-wave form, which is given by

$$V_{\rm pq} = \frac{1}{r_{\rm pq}} = \sum_{l=0}^{\infty} \frac{r_<^l}{r_>^{l+1}} {\rm P}_l(\cos\theta). \tag{6}$$

where $r_{\rm pq} = |\boldsymbol{r}_{\rm p} - \boldsymbol{r}_{\rm q}|$, $r_> = \max(r_{\rm p}, r_{\rm q})$, $r_< = \min(r_{\rm p}, r_{\rm q})$, and $P_l$ are the Legendre polynomials. The SDH potential of the CB interaction is modified as[23]

$$V_{\rm pq} = \frac{1}{r_{\rm pq}} \exp\left(\frac{-r_{\rm q}}{D}\right) = \sum_{l=0}^{\infty} \frac{r_<^l}{r_>^{l+1}} \exp\left(\frac{-r_{\rm q}}{D}\right) {\rm P}_l(\cos\theta), \tag{7}$$

and the NSDH one is written as[35]

$$\begin{aligned} V_{\rm pq} &= \frac{1}{r_{\rm pq}} \exp\left(\frac{-r_{\rm pq}}{D}\right) \\ &= -\frac{1}{D} \sum_{l=0}^{\infty} (2l+1) {\rm j}_l\left(\frac{{\rm i}r_<}{D}\right) {\rm h}_l^{(1)}\left(\frac{{\rm i}r_>}{D}\right) {\rm P}_l(\cos\theta), \end{aligned} \tag{8}$$

where $\rm j_l$ and $\rm h_l^{(1)}$ are the spherical Bessel and Hankel functions of the first kind with complex arguments, respectively. As $D \rightarrow \infty$, equations (7) and (8) reduce to the unscreened Eq. (6).

In Eqs. (4) and (5), the bound target wavefunctions are obtained by means of the MCDF method, in which the atomic state wavefunction is represented as a linear combination of configuration state wavefunctions.[36] In order to include the plasma-screening effect on the target ion (changes of target wavefunctions due to Debye screening), the MCDF calculations were performed by the GRASP2K program[37] with some modifications,[35] in which the DH potential is incorporated into the relativistic Hamiltonian. The MCDF method including the Debye-screening effect has been described in detail by Xie *et al.*[35] as well as Saha and Fritzsche.[38] The distorted-wave wavefunctions of the continuum electron are obtained by solving the coupled Dirac equations numerically.[36] The numerical procedures are accomplished by using the component

COWF of RATIP,[39] in which the two-body Coulomb potential (6) has been modified by replacement with the screened ones (7) and (8) for the SDH and NSDH potentials, respectively. Moreover, the Debye-screened electron–nucleus potential is considered as $V_{\rm nuc}(r) = -(Z/r)\exp(-r/D)$. In addition, the asymptotic continuum wavefunctions are determined numerically for the boundary conditions, based on the WKB method.[40]

## 3. Results and discussion

The Yukawa-type screened potential (1) has been often utilized for the theoretical studies of atomic structures and collision dynamics in weakly coupled plasmas, but Chang and Fang[41] pointed out that the Debye-screening length should be longer than the average size of a free atom, as the mean radius of the 2p orbital in an $N^{5+}$ ion was estimated to be $\sim 0.4$ a.u. (atomic units). Moreover, the DH potential supports only a finite number of bound states, which results in a migration of the bound state into the continuum when $D$ is less than the critical screening length.[42] According to the work of Xie *et al.*,[35] the critical screening length was determined to be 0.93 a.u. for the state 1s2p $^1$P in a He-like $C^{4+}$ ion. Therefore, the range of the screening length was chosen as from 1 a.u. to $\infty$ so that the 1s2p $^1$P in $Al^{11+}$ and $Fe^{24+}$ ions is still the bound state. Due to weak electron correlations in the present cases of highly charged He-like ions, the single-configuration approximation is employed.

### 3.1. Test of numerical methods

In order to verify the numerical methods and computing codes, the present EIE cross sections for the transition 1s $\rightarrow$ 2p in an $Ne^{9+}$ ion are compared with the distorted-wave calculations[23] for $D = 3$ a.u. with the SDH potential in Fig. 1, and a good agreement is obtained. As a check of our numerical methods, which includes the Debye screening on both the target ions and the CB interaction with NSDH potential, our RDW results are compared with the 110-state CCC calculations[28] for the transition $1s^2\ ^1S \rightarrow 1s2p\ ^1P$ in He in Fig. 2. It is noted that our purpose is not to discuss the accuracy of the RDW method for calculating the EIE cross section of a neutral He atom, but to characterize the plasma-screening effect. It is found that at the high incident electron energy of 800 eV, both of the present unscreened and screened ($D = 10$ a.u.) calculations nearly agree with the CCC calculations, which supports the reliability of our theoretical method and codes used to include Debye-screening effects on EIE processes.

### 3.2. Transition energy and oscillator strength

Table 1 shows the Debye-screening effect on the transition energy and oscillator strength for the dipole-allowed transition $1s^2\ ^1S \rightarrow 1s2p\ ^1P$ in $Al^{13+}$ and $Fe^{24+}$ ions. Generally, when the screening length $D$ is sufficiently greater than the radius of the ions, the influence of the Debye screening can be neglected. For the case of $D \rightarrow \infty$, the present transition energy agrees well with the NIST value[43] with differences of 0.09% and 0.11% for $Al^{13+}$ and $Fe^{24+}$ ions, respectively. Moreover, the relative differences between our unscreened oscillator strengths and the NIST data[43] are determined to be 5.37% and 0.57% for $Al^{13+}$ and $Fe^{24+}$ ions, respectively. This indicates the reliability of the single-configuration approximation employed in the present calculations. As expected, when the screening length $D$ is comparable to the radius of ions, the Debye-screening effect strongly affects the atomic properties. Thus, in Table 1 the screening effect makes significant reductions in the transition energy and oscillator strength when $D$ is smaller than about 5 a.u., while the screening effect is very small for the case of $D > 10$ a.u.

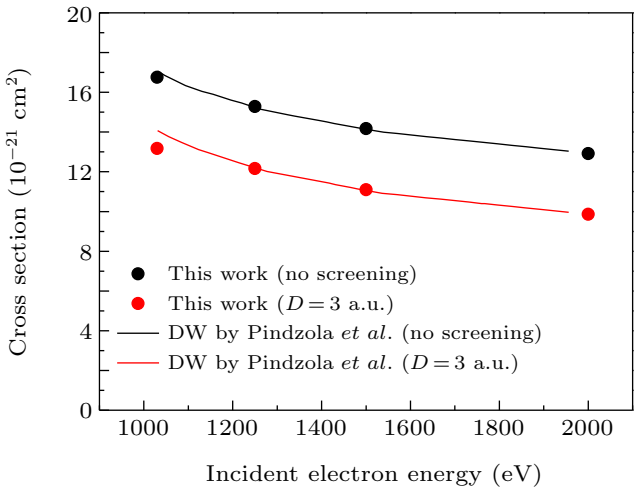



**Fig. 1.** Comparison of the present unscreened and screened EIE cross sections for the transition 1s $\rightarrow$ 2p of $Ne^{9+}$ ion with those of the distorted-wave (DW) calculations by Pindzola *et al.*[23] The screened results for $D = 3$ a.u. consider the bound-continuum interaction by the SDH potential.

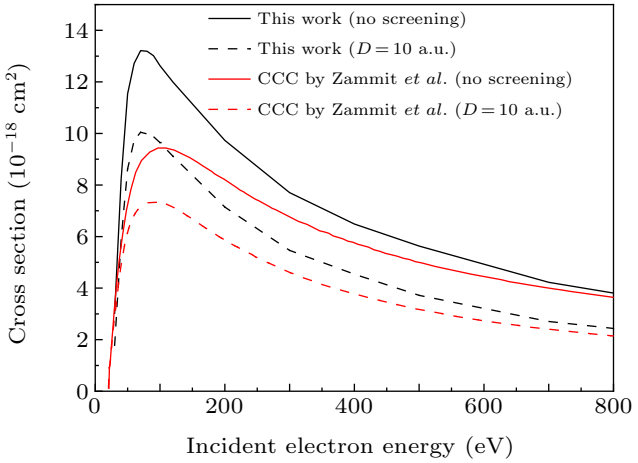



**Fig. 2.** Comparison of the present unscreened and screened EIE cross sections for the transition $1s^2\ ^1S \rightarrow 1s2p\ ^1P$ in He with those of the 110-state CCC calculations by Zammit *et al.*[28] The screened results for $D = 10$ a.u. consider the plasma screening on both the target ion and interaction between the continuum electron and bound electron with the NSDH potential.

**Table 1.** Transition energy (eV) and oscillator strength for the transition $1s^2\ ^1S \rightarrow 1s2p\ ^1P$ in $Al^{13+}$ and $Fe^{24+}$ ions for screening length $D$ (a.u.).

| $D$ | $Al^{11+}$ | | $Fe^{24+}$ | |
|---|---|---|---|---|
| | Transition energy | Oscillator strength ($10^{-1}$) | Transition energy | Oscillator strength |
| $\infty$ | 1596.85 | 7.053 | 6707.49 | 6.954 |
| | 1598.29[a] | 7.45[a] | 6700.42[a] | 7.04[a] |
| 100 | 1596.85 | 7.053 | 6707.48 | 6.954 |
| 50 | 1596.84 | 7.053 | 6707.47 | 6.954 |
| 15 | 1596.64 | 7.049 | 6707.27 | 6.954 |
| 12.5 | 1596.55 | 7.048 | 6707.18 | 6.953 |
| 1 | 1596.38 | 7.045 | 6707.01 | 6.953 |
| 8 | 1596.11 | 7.040 | 6706.74 | 6.952 |
| 5 | 1594.97 | 7.021 | 6705.60 | 6.947 |
| 2.5 | 1589.58 | 6.931 | 6700.07 | 6.927 |
| 1.25 | 1569.50 | 6.602 | 6678.83 | 6.849 |
| 1 | 1555.24 | 6.369 | 6663.42 | 6.793 |

[a]Unscreened values from NIST.[43]

### 3.3. Cross section

Next, we investigate the Debye-screening effect on the EIE cross sections for the transition $1s^2\ ^1S \rightarrow 1s2p\ ^1P$ in He-like $Al^{11+}$ and $Fe^{24+}$ ions. In Fig. 3, the variations of the EIE cross section at incident energies of 3000 eV and 15000 eV are illustrated for $Al^{11+}$ and $Fe^{24+}$ ions, respectively, with SDH and NSDH potentials. The variation $\Delta\sigma$ is defined as the difference between the cross section with the pure Coulomb interaction and that with the Debye-screened case, i.e., $\Delta\sigma = \sigma(D \rightarrow \infty) - \sigma(D > 0)$. As shown in Fig. 3, since $\Delta\sigma$ is always positive, the Debye-screening effect decreases the EIE cross sections. Moreover, the $\Delta\sigma$ becomes more obvious with decreasing $D$. It is noted that variations $\Delta\sigma$ of the SDH potential are dramatically greater than those of the NSDH potential, except that the Debye screening is weak in the large-$D$ cases. Thus, the SDH model can significantly overestimate the Debye-screening effects.

When the Debye-screening effect on the target ion is considered, the EIE cross sections decrease further, which is demonstrated in Fig. 3. However, for about $D > 5$ a.u., the variations of the EIE cross section are almost the same as in the case in which the Debye screening on the target ion is not included. This indicates that the screening imposed on the target ion has negligible contributions to the EIE cross section when the plasma screening is too weak to affect the target ions for cases of $D > 5$ a.u.

We define the ratio

$$R = \frac{\sigma_{\rm ion}(D)}{\sigma_{\rm ee}(D)}, \tag{9}$$

where $\sigma_{\rm ion}(D)$ and $\sigma_{\rm ee}(D)$ represent the contributions from the Debye screening on the target ion and CB interaction, respectively, for reducing the EIE cross section. Here, the screened CB interaction is described by the NSDH model. In Fig. 4, since the ratio $R$ is always less than one for all the screening length, the screening on the CB interaction is dominant for affecting (reducing) the EIE cross sections for the transition $1s^2\ ^1S \rightarrow 1s2p\ ^1P$ in $Al^{11+}$ and $Fe^{24+}$ ions at the incident energies of 3000 eV and 15000 eV, respectively. Moreover, as the screening length decreases, the influence of the Debye screening on the target ion increases (the ratio $R$ increases). As shown in Fig. 4, in the case of $D = 1$ a.u., $R \sim 0.24$ and 0.18 for $Al^{11+}$ and $Fe^{24+}$ ions, respectively; hence, it indicates that the influences of screening on the target ion should be included for strong plasma screening. On the other hand, for the screening length $D = 10$ a.u., the ratio is estimated to be $R \sim 0.05$ and 0.03 for the $Al^{11+}$ and $Fe^{24+}$ cases, respectively, which implies that the reductions of the EIE cross sections are almost determined by the screening on the CB interaction. This also results in the fact that the influences of screening on the target ion are negligible for sufficiently weak screening strength, which will be demonstrated further in Fig. 5.

In Fig. 5, the screened ($D = 10$ a.u.) and unscreened EIE cross sections are shown for the transition $1s^2\ ^1S \rightarrow 1s2p\ ^1P$ in He-like $Al^{11+}$ ions at different incident energies. In the process of the electron–ion collision, the cross sections at the threshold are finite since the long-range Coulomb interaction has contributions to the large separation between the continuum electron and target ion. Thus, the EIE cross sections at the threshold should be more significantly reduced due to the short-range character of the DH potential with the exponential screening factor [see Eq. (1)]. However, in Fig. 5 the reductions of the EIE cross section due to the SDH potential are basically the same for incident energy ranging from the threshold to high energy. For the NSDH potential, it clearly demonstrates that the reductions of the cross section at the threshold are indeed larger than those at high energies. Hence, the NSDH potential could reasonably describe the Debye-screening effects on the EIE process in Debye plasmas, as expected since this potential results in a reasonable changing behavior of the cross section with incident energy.

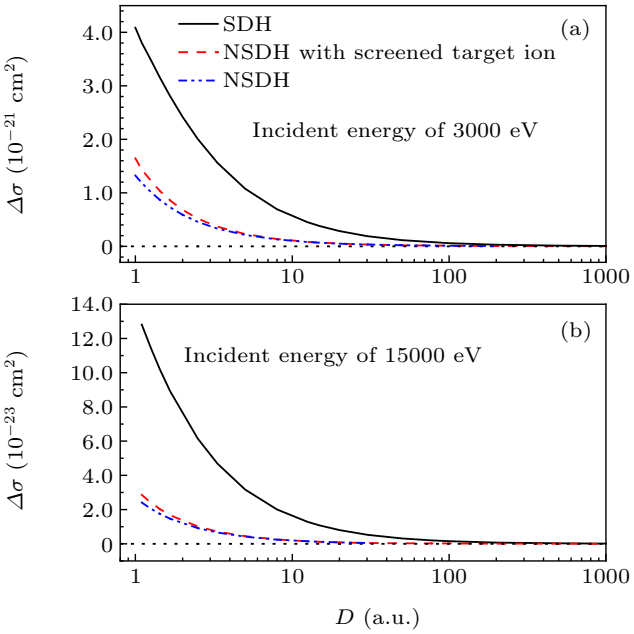



**Fig. 3.** Variation of the EIE cross section, $\Delta\sigma = \sigma(D \to \infty) - \sigma(D > 0)$, for the transition $1s^2\ ^1S \to 1s2p\ ^1P$ in $Al^{11+}$ (a) and $Fe^{24+}$ (b) ions, respectively. SHD and NSDH [see Eqs. (2)–(3) and text] indicate that the CB interaction is described by the SDH and NSDH potentials, respectively. NSDH with screened target ion means that Debye screening on the target ion is included as well.

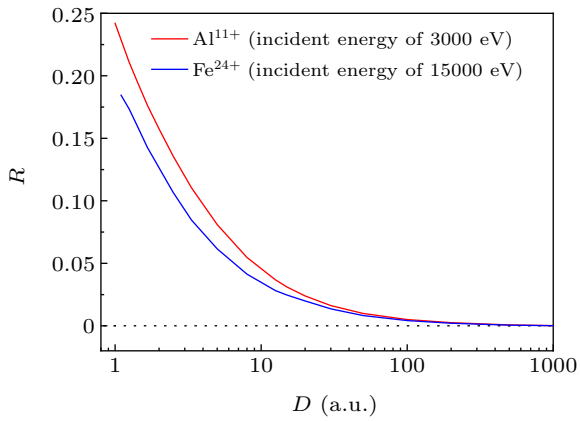



**Fig. 4.** Ratio $R$ [see Eq. (9) and text] for the transition $1s^2\ ^1S \to 1s2p\ ^1P$ in $Al^{11+}$ and $Fe^{24+}$ ions, respectively.

Moreover, as mentioned above, in Fig. 3 the ratio $R$at the incident electron energy of 3000 eV is shown for a He-like $Al^{11+}$ ion, which is estimated to be $\sim 0.05$ for the case of $D = 10$ a.u., indicating that the screening on the target ion results in negligible reductions of the cross sections compared to the screening on the CB interaction. As illustrated in Fig. 5, this is also true for the energy range from threshold to 10000 eV, since there are no significant differences between the cross sections with and without inclusions of the screening on the target ion for $D = 10$ a.u.

In Fig. 6, the EIE cross sections are displayed for the dipole-allowed transition $1s^2\ ^1S \to 1s2p\ ^1P$ in He-like $Al^{11+}$ and $Fe^{24+}$ ions with $D = \infty$, 5, 2, and 1 a.u. For the unscreened EIE cross sections, our results agree with the available theoretical calculations by Kieffer *et al.*,[44] Hakel *et al.*[45] and Zhang *et al.*[33] The EIE cross sections are decreased due to Debye-screening effects, which become distinct with decreasing $D$. For example, at the incident energy of 3400 eV, the EIE cross section is reduced by about 13.4%, 30.2%, and 50.9% for $D = 5$, 2, and 1 a.u., respectively, for He-like $Al^{11+}$ ions. Moreover, the screening effect decreases the cross section by about 3.1%, 7.8%, and 15.6% for $D = 5$, 2, and 1 a.u., respectively, near the threshold of 7500 eV for He-like $Fe^{24+}$ ions.

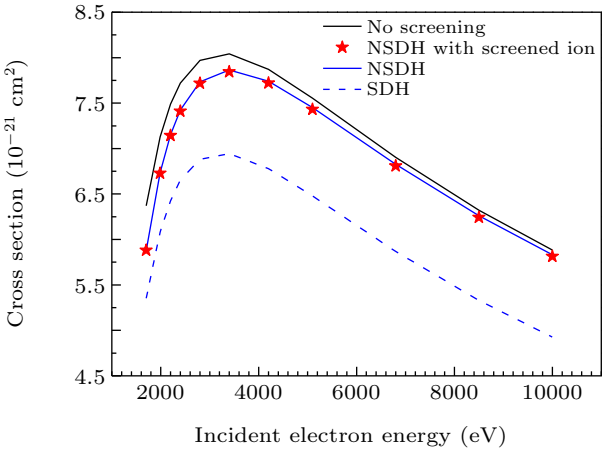



**Fig. 5.** Unscreened (black line) and screened ($D = 10$ a.u.) EIE cross sections for the transition $1s^2\ ^1S \to 1s2p\ ^1P$ in $Al^{11+}$ ions. SHD and NSDH [see Eqs. (2)–(3) and text] indicate that the CB interaction is described by the SDH and NSDH potentials, respectively. NSDH with screened target ion means that Debye screening on the target ion is included as well.

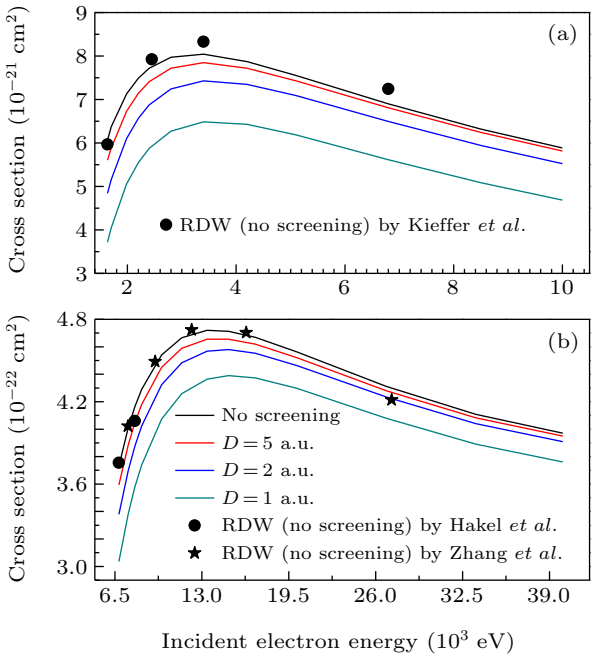



**Fig. 6.** EIE cross sections for the transition $1s^2\ ^1S \to 1s2p\ ^1P$ in $Al^{11+}$ (a) and $Fe^{24+}$ (b) ions with the screening length $D = \infty$, 5, 2, and 1 a.u. Present unscreened cross sections are compared with the available RDW results by Kieffer *et al.*,[44] Zhang *et al.*,[33] and Hakel *et al.*[45]

## 4. Conclusion

We have studied the EIE processes for the dipole-allowed transition $1s^2\ ^1S \to 1s2p\ ^1P$ in He-like $Al^{11+}$ and $Fe^{24+}$ ions embedded in weakly coupled (Debye) plasmas using the

MCDF and RDW methods with the DH potential. In order to account for the Debye-screening effect on the CB interaction in the EIE process, two model potentials (SDH and NSDH) are employed, which result in reductions of the EIE cross section. However, the reduced magnitude of the EIE cross sections for the SDH potential is far greater than that for the NSDH potential. Therefore, the well-suited SDH potential obviously overestimates the Debye-screening effects on the EIE processes for multielectron He-like ions. Moreover, the Debye-screening effect on the target ion also decreases the EIE cross sections. Our results reveal that the influence of the screening on the CB interaction is dominant for the reduction of the EIE cross section, while the screening on the target ion could contribute to reducing the cross sections further as the screening strength increases. However, for cases of sufficiently weak screening strength, the contributions of the screening on the target ion are negligible.

Finally, the EIE cross sections are presented with the inclusion of the Debye-screening effect on both the target ion and the CB interaction. It is found that the Debye-screening effects obviously reduce the EIE cross sections, which clearly indicates that atomic processes are perturbed in a non-negligible way in plasmas. Therefore, it is highly desirable to investigate environmental effects on plasma kinetics, as well as on absorption and emission spectra.

## Acknowledgments

Project supported by the Science Challenge Project (Grant No. TZ2016001), the National Key Research and Development Program of China (Grants Nos. 2017YFA0403200 and 2017YFA0402300), the Funds for Innovative Fundamental Research Group Project of Gansu Province, China (Grant No. 20JR5RA541), and the National Natural Science Foundation of China (Grants Nos. 11774037 and 12064041).

## References

[1] Heeter R F, Hansen S B, Fournier K B, Foord M E, Froula D H, Mackinnon A J, May M J, Schneider M B and Young B K F 2007 *Phys. Rev. Lett.* **99** 195001
[2] Gao C, Jin F, Zeng J and Yuan J 2013 *New J. Phys.* **15** 015022
[3] Chintan S, Pedro A, René S, Sven B, José R C L U and Stanislav T 2018 *Astrophys. J. Suppl. Ser.* **234** 27
[4] Shah C, Amaro P, Steinbrügge R, Beilmann C, Bernitt S, Fritzsche S, Surzhykov A, Crespo López-Urrutia J R and Tashenov S 2016 *Phys. Rev. E* **93** 061201
[5] Belkhiri M and Poirier M 2014 *Phys. Rev. A* **90** 062712
[6] Ichimaru S 1982 *Rev. Mod. Phys.* **54** 1017
[7] Whitten B L, Lane N F and Weisheit J C 1984 *Phys. Rev. A* **29** 945
[8] Belkhiri M and Fontes C J 2016 *J. Phys. B* **49** 175002
[9] Zhang D H, Xie L Y, Jiang J and Dong C Z 2019 *Chin. Phys. Lett.* **36** 083401
[10] Weisheit J C 1989 *Adv. At. Mol. Phys.* **25** 101
[11] Murillo M S and Weisheit J C 1998 *Phys. Rep.* **302** 1
[12] Janev R K, Zhang S and Wang J 2016 *Matter Radiat. Extremes* **1** 237
[13] Yoon J S and Jung Y D 1996 *Phys. Plasmas* **3** 3291
[14] Ma J, Wang Y C, Zhou Y J and Wang H 2018 *Chin. Phys. B* **27** 013401
[15] Zhang S B, Qi Y Y, Qu Y Z, Chen X J and Wang J G 2010 *Chin. Phys. Lett.* **27** 013401
[16] Hatton G J, Lane N F and Weisheit J C 1981 *J. Phys. B* **14** 4879
[17] Scheibner K, Weisheit J C and Lane N F 1987 *Phys. Rev. A* **35** 1252
[18] Li B W, Dong C Z, Jiang J and Wang J G 2010 *Eur. Phys. J. D* **59** 201
[19] Jiang J, Dong C Z and Xie L Y 2014 *Chin. Phys. Lett.* **31** 023401
[20] Chen Z B, Dong C Z, Jiang J and Xie L Y 2015 *J. Phys. B* **48** 144030
[21] Chen Z 2018 *Phys. Plasmas* **25** 052105
[22] Qi Y Y, Ye D D, Wang J G and Qu Y Z 2015 *Chin. Phys. B* **24** 033403
[23] Pindzola M S, Loch S D, Colgan J and Fontes C J 2008 *Phys. Rev. A* **77** 062707
[24] Zhang S B, Wang J G and Janev R K 2010 *Phys. Rev. Lett.* **104** 023203
[25] Zhang S B, Wang J G and Janev R K 2010 *Phys. Rev. A* **81** 032707
[26] Zhang S B, Wang J G, Janev R K and Chen X J 2011 *Phys. Rev. A* **83** 032724
[27] Zammit M C, Fursa D V and Bray I 2010 *Phys. Rev. A* **82** 052705
[28] Zammit M C, Fursa D V and Bray I 2012 *Chem. Phys.* **398** 214
[29] Zammit M C, Fursa D V, Bray I and Janev R K 2011 *Phys. Rev. A* **84** 052705
[30] Zhou F Y, Qu Y Z, Gao J W, Ma Y L, Wu Y and Wang J G 2021 *Commun. Phys.* **4** 148
[31] Stillman C R, Nilson P M, Ivancic S T, Golovkin I E, Mileham C, Begishev I A and Froula D H 2010 *Phys. Rev. E* **95** 063204
[32] Jiang J, Dong C Z, Xie L Y and Wang J G 2008 *Phys. Rev. A* **78** 022709
[33] Zhang H L, Sampson D H and Clark R E H 1990 *Phys. Rev. A* **41** 198
[34] Bar-Shalom A, Klapisch M and Oreg J 1988 *Phys. Rev. A* **38** 1773
[35] Xie L Y, Wang J G, Janev R K, Qu Y Z and Dong C Z 2012 *Eur. Phys. J. D* **66** 125
[36] Dyall K G, Grant I P, Johnson C T, Parpia F A and Plummer E P 1989 *Comput. Phys. Commun.* **55** 425
[37] Jönsson P, He X, Froese Fischer C and Grant I P 2007 *Comput. Phys. Commun.* **177** 597
[38] Saha B and Fritzsche S 2006 *Phys. Rev. E* **73** 036405
[39] Fritzsche S, Aksela H, Dong C Z, Heinäsmäki S and Sienkiewicz J E 2003 *Nucl. Instrum. Methods Phys. Res. B* **205** 93
[40] Ong W and Russek A 1978 *Phys. Rev. A* **17** 120
[41] Chang T N and Fang T K 2013 *Phys. Rev. A* **88** 023406
[42] Qi Y Y, Wang J G and Janev R K 2009 *Phys. Rev. A* **80** 063404
[43] Kramida A, Ralchenko Yu, Reader J and NIST ASD Team 2020 *NIST Atomic Spectra Database* (ver. 5.8), May 28, 2021, National Institute of Standards and Technology, Gaithersburg, MD
[44] Kieffer J C, Matte J P, Chaker M, Beaudoin Y, Chien C Y, Coe S, Mourou G, Dubau J and Inal M K 1993 *Phys. Rev. E* **48** 4648
[45] Hakel P, Mancini R C, Harris C, Neill P, Beiersdorfer P, Csanak G and Zhang H L 2007 *Phys. Rev. A* **76** 012716